UNINTEGRATED PARTON DISTRIBUTIONS AND APPLICATIONS TO JET PHYSICS*

F. Hautmann

Theoretical Physics Department, University of Oxford
Oxford OX1 3NP, UK

(Received May 28, 2009)

We give a concise overview on unintegrated parton distributions and discuss applications to the physics of parton showers and hadronic jets.

PACS numbers: 12.38.–t, 13.87.–a

1. Introduction

The interpretation of experimental data for multi-particle final states at the Large Hadron Collider will rely both on perturbative calculations for multi-leg scattering amplitudes and on realistic event simulation by parton-shower Monte Carlo generators.

Owing to the complex kinematics involving multiple hard scales and the large phase-space opening up at very high energies, high-multiplicity events are potentially sensitive to effects of QCD initial-state radiation that depend on the finite transverse-momentum tail of partonic matrix elements and distributions. These effects are not included in the branching algorithms of standard shower Monte Carlo event generators, based on collinear jet evolution. On the other hand, they are taken into account only partially in perturbative fixed-order calculations, order-by-order through higher-loop contributions. Such effects are present to all orders in α_s and can become logarithmically enhanced at high energy.

The phenomenological significance of finite-$k_\perp$ corrections to parton showers is largely associated with effects of coherence of multiple gluon emission for small parton momentum fractions. This article focuses on the formulation of these effects in a manner suitable for Monte Carlo calculations, by using coherent-branching methods based on unintegrated parton distributions and matrix elements.

* Presented at the Cracow Epiphany Conference on Hadron Interactions at the Dawn of the LHC, Cracow, Poland, January 5–7, 2009.

We start in Sec. 2 by briefly reviewing the main principles of parton-branching approaches. In Sec. 3 we discuss current progress in the theory of unintegrated pdfs. In Sec. 4 we consider jet physics applications.

2. Multi-parton emission by parton branching methods

Given a full high-energy *pp* collision event, consisting of a hard scatter, parton showering, hadronization and soft underlying process (Fig. 1), we will concentrate on the part — hard event and showering — that can be understood by perturbative treatment. The main focus of this section is on the description of multi-parton emission by branching methods.

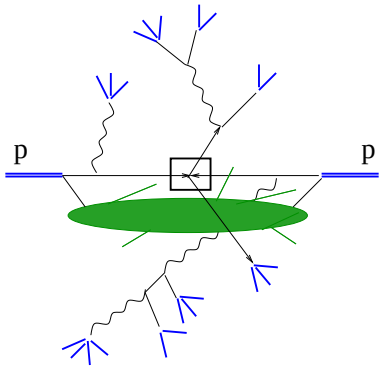

Fig. 1. A high-energy *pp* collision event.

2.1. Collinear approximation

Branching algorithms in standard shower Monte Carlo generators [1] are based on collinear evolution of the jets developing, both "forwards" and "backwards", from the hard event. The branching probability is given in terms of splitting functions P and form factors Δ (Fig. 2) as

$$d\mathcal{P} = \int \frac{dq^2}{q^2} \int dz\, \alpha_{\rm S}\left(q^2\right)\, P(z) \Delta\left(q^2, q_0^2\right) . \tag{1}$$

The theoretical basis for the branching approach is the factorizability of universal splitting functions in QCD cross-sections in the collinear limit [2,3], which justifies the probabilistic picture.

Besides small-angle, incoherent parton emission, shower generators (or more precisely some of them, see *e.g.* discussions in [4, 5]) also take into account further radiative contributions, associated with emission of soft gluons. These contributions are essential for realistic phenomenology [4, 5]. To incorporate them in a probabilistic framework, one appeals to properties of coherence of color charge radiation.

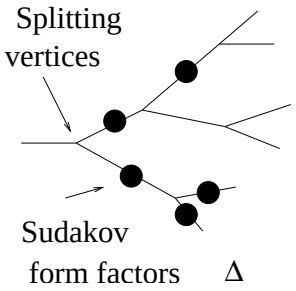

Fig. 2. Parton branching in terms of splitting probabilities and form factors.

2.2. Soft gluon coherence

Recall [2, 6, 7] that soft-gluon emission amplitudes factorize in terms of eikonal currents [8, 9]

$$\boldsymbol{J}^a_\mu = \sum_{i=1}^{n} \boldsymbol{Q}^a_i \frac{p_{i\mu}}{p_i \cdot q}\,, \tag{2}$$

where p_i are the emitters' momenta, q is the soft momentum, and the color charge operators $\boldsymbol{Q}^a_i$ are associated with the emission of gluon a from parton i. In general, interferences are expected to contribute to the radiative terms relating the $(n+1)$-parton process to the n-parton process,

$$d\sigma_{n+1} = d\sigma_n \, \frac{d^3q}{(q^0)^3} \sum_{i,j} \boldsymbol{Q}_i \cdot \boldsymbol{Q}_j w_{ij}\,, \qquad w_{ij} = \frac{(q^0)^2 \; p_i \cdot p_j}{(p_i \cdot q)(p_j \cdot q)}\,. \tag{3}$$

Nevertheless, a probabilistic branching-like picture can be recovered [10–12] by exploiting soft-gluon coherence.

At the single-emission level, this can be described simply as a property of azimuthal averages of the radiation function w_{ij} in (3). To this end use the identity

$$\begin{aligned} \left(q^0\right)^2 \; \frac{p_i \cdot p_j}{p_i \cdot q \; p_j \cdot q} \; &\equiv \; \frac{\zeta_{ij}}{\zeta_{iq}\zeta_{jq}} \\ &= \; \frac{1}{2}\left(\frac{\zeta_{ij}}{\zeta_{iq}\zeta_{jq}} - \frac{1}{\zeta_{jq}} + \frac{1}{\zeta_{iq}}\right) + \frac{1}{2}\left(\frac{\zeta_{ij}}{\zeta_{iq}\zeta_{jq} - \frac{1}{\zeta_{iq}} + \frac{1}{\zeta_{jq}}}\right)\,, \end{aligned} \tag{4}$$

in Eq. (3), where for each momentum pair we have set

$$\zeta_{nk} \equiv \frac{p_n \cdot p_k}{p^0_n p^0_k} \overset{m\to 0}{\simeq} 1 - \cos\theta_{nk}\,, \tag{5}$$

and take the azimuthal average for each of the two terms in the second line of Eq. (4) separately. This gives

$$\left\langle \frac{\zeta_{ij}}{\zeta_{iq}\zeta_{jq}} \right\rangle = \frac{1}{\zeta_{iq}}\Theta(\zeta_{ij}-\zeta_{iq}) + \frac{1}{\zeta_{jq}}\Theta(\zeta_{ij}-\zeta_{jq})\,. \tag{6}$$

Eq. (6) is the sum of a term for emission from parton i and a term for emission from parton j, each with the new constraint that no radiation is emitted at angles larger than the angle between the two emitters (Fig. 3). For suitably averaged distributions, the net effect of interferences is effectively to cancel the radiation outside the angular region between the directions of the emitters, leaving a quasiclassical-looking formula.

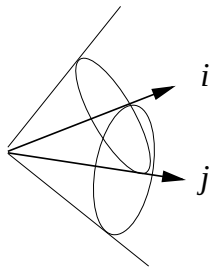

Fig. 3. Emission cones around the directions of the emitters.

The main point is that an extension of this mechanism iterates to multiple emissions. The next simplest case is depicted in Fig. 4 with production of two soft gluons, of momenta q_1 and q_2, from a fast parton of momentum p (Fig. 4(a)). Suppose $q_2^0 \ll q_1^0$, and consider the currents for radiating q_1 from p, and q_2 from p and q_1,

$$\boldsymbol{J}_1^{\mu a_1} = \boldsymbol{Q}_p^{a_1}\frac{p^\mu}{p\cdot q_1}\,, \qquad \boldsymbol{J}_2^{\mu a_2} = \boldsymbol{Q}_p^{a_2}\frac{p^\mu}{p\cdot q_2} + \boldsymbol{Q}_{q_1}^{a_2}\frac{q_1^\mu}{q_1\cdot q_2}\,. \tag{7}$$

By evaluating the action of the charge operators on the parton states, the gluon emission amplitude for the transition of the fast-parton state is

$$\begin{aligned}\mathcal{M}_{ki}^{a_1 a_2} &= g_s^2\,\langle a_1 k|\boldsymbol{J}_2\cdot\varepsilon_2|a'\,i'\rangle\,\langle i'|\boldsymbol{J}_1\cdot\varepsilon_1|i\rangle \\ &= g_s^2\frac{p\cdot\varepsilon_1}{p\cdot q_1}\left(\frac{p\cdot\varepsilon_2}{p\cdot q_2}t^{a_2}t^{a_1} + \frac{q_1\cdot\varepsilon_2}{q_1\cdot q_2}\,[t^{a_1},t^{a_2}]\right)_{ki}\,.\end{aligned} \tag{8}$$

We can distinguish two angular regions for the softest gluon q_2 in Eq. (8). *(i)* When q_2 is at small angle from p (q_1), then the first (second) term dominates the quantity in the brackets in Eq. (8), and the amplitude can be seen as the sequential emission of q_1 from p and of q_2 from p (q_1). This

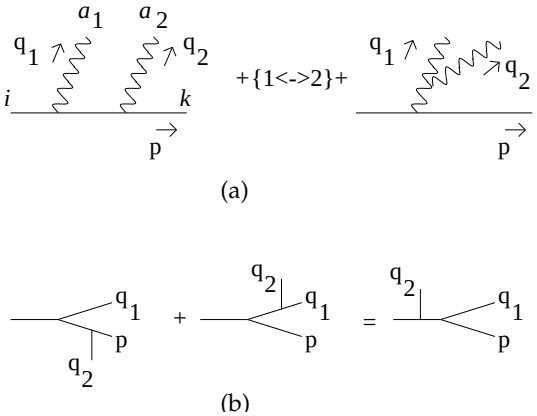

Fig. 4. (a) Two gluon emission from a fast quark; (b) coherence of soft gluon emission at large angle.

corresponds to the standard bremsstrahlung picture based on radiation cones centered around p and q_1. *(ii)* When q_2 is at large angle, $\theta_{pq_2} \gg \theta_{pq_1}$, then the directions of p and q_1 can be identified and the two emission amplitudes act coherently to give

$$\mathcal{M}^{a_1 a_2} \simeq g_s^2 \frac{p \cdot \varepsilon_1}{p \cdot q_1} \frac{p \cdot \varepsilon_2}{p \cdot q_2} t^{a_1} t^{a_2} , \tag{9}$$

which can be seen as the sequential emission of q_2 from p and of q_1 from p. This is pictured in Fig. 4(b). The reversed order of the emissions compared to case *(i)* comes from the color algebra and reflects the fact that the radiated gluon sees the total color charge of the emitting jet.

Fig. 4(b) illustrates that the contributions of different emitters combine so as to give an effective contribution in which the emissions are ordered in angle. Angular ordering thus replaces energy ordering: in the right hand side of Fig. 4(b) the gluon emitted first is no longer the hardest.

The phenomenological relevance of these contributions has been emphasized over the years by extensive collider data studies. An example based on recent Tevatron data for $p\bar{p}$ jet fragmentation is shown in Fig. 5 [1]. Quantitative effects of color coherence are illustrated by comparing theory predictions with and without coherence against di-jet Tevatron data and earlier e^+e^- and ep data.

2.3. Spacelike jet at high energies

The arguments used in the previous subsection take into account, through the currents (2), (3), soft vector emission from external lines in parton scattering amplitudes, and are fully appropriate for scattering problems characterized by a single hard scale [2]. In processes with multiple hard scales, on

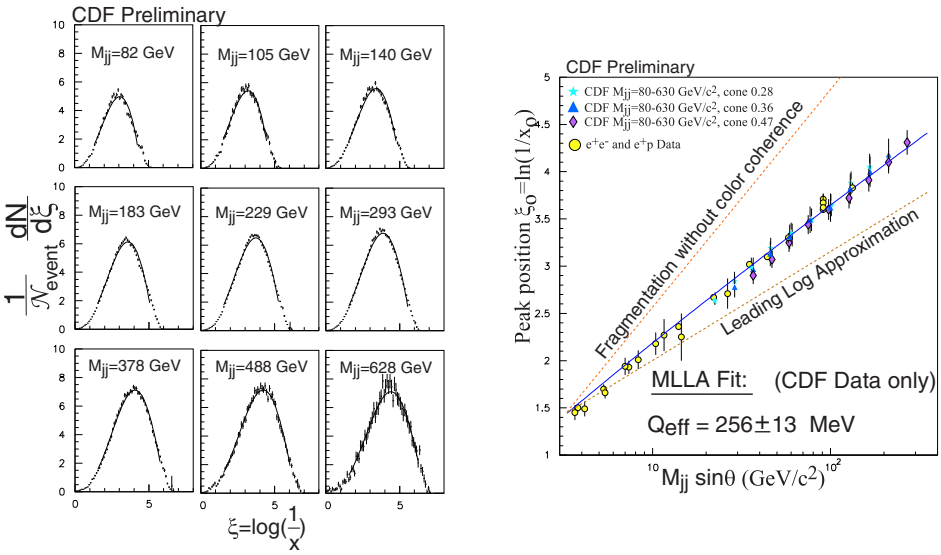

Fig. 5. Comparison [1] of predictions including soft-gluon coherence with jet fragmentation data at the Tevatron.

the other hand, emissions in the parton branching that are not collinearly ordered become non-negligible. Coherence sets in from emissions due to internal lines in the branching decay chain, involving space-like partons (Fig. 6) possibly carrying small longitudinal momentum fractions. As the phase-space opens up for multi-scale hard events at LHC energies, it becomes increasingly relevant to investigate such effects.

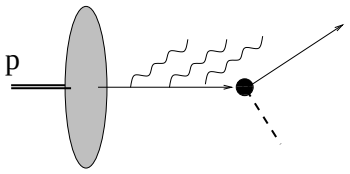

Fig. 6. Spacelike jet evolution.

Soft-gluon recursion relations and corresponding factorization formulas in the high-energy kinematics can be given in terms of real and virtual soft-gluon currents [13–17]

$$|M^{(n+1)}(k,p)|^2 = \left\{ \left[M^{(n)}(k+q,p)\right]^\dagger \left[\boldsymbol{J}^{(\mathrm{R})}\right]^2 M^{(n)}(k+q,p) - \left[M^{(n)}(k,p)\right]^\dagger \left[\boldsymbol{J}^{(\mathrm{V})}\right]^2 M^{(n)}(k,p) \right\}, \qquad (10)$$

but the structure of these relations is more complex than in the case of soft emissions from external lines. More precisely, the currents depend on the transverse momentum transmitted down the decay chain, and virtual processes are not simply represented by incorporating Sudakov form factors in the branching [13]. Factorization holds in terms of partonic distributions and matrix elements unintegrated in both longitudinal and transverse momenta [14].

The resulting branching equations differ from the structure in Eq. (1): the branching probability is $k_\perp$-dependent, and part of the virtual corrections are associated to the (unintegrated) splitting functions. Schematically one has, using the recursion relation (10),

$$\mathcal{G}(x,k_\perp,\mu) \;=\; \mathcal{G}_0(x,k_\perp,\mu) + \int \frac{dz}{z} \int \frac{dq^2}{q^2}\,\Theta(\mu - zq) \times \Delta(\mu,zq)\,\mathcal{P}(z,q,k_\perp)\,\mathcal{G}\left(\frac{x}{z}, k_\perp + (1-z)q, q\right)\,, \quad (11)$$

where $\mathcal{G}$ is the unintegrated gluon distribution, Δ is the form factor, and $\mathcal{P}$ is the unintegrated splitting function (Fig. 7). In this picture $\mathcal{P}$ depends on transverse momenta and includes part of the virtual corrections, in such a way as to avoid double counting with the Sudakov form factor Δ, while reconstructing color coherence not only at large x but also at small x [18] in the angular region (Fig. 7)

$$\frac{\alpha}{x} > \alpha_1 > \alpha\,, \quad (12)$$

where the angles α for the partons radiated from the initial-state shower are taken with respect to the initial beam jet direction, and increase with increasing off-shellness.

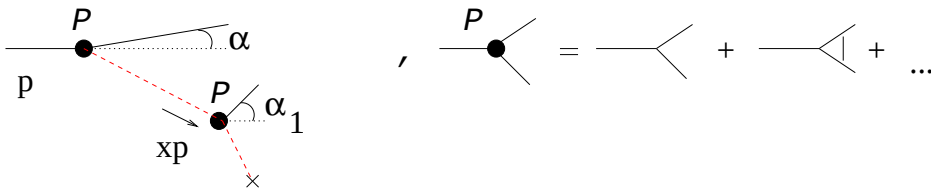

Fig. 7. (Left) Coherent radiation in the space-like parton shower for $x \ll 1$; (right) the unintegrated splitting function $\mathcal{P}$, including small-x virtual corrections.

From the standpoint of higher-order corrections, the effects of region (12) are potentially enhanced by terms

$$\alpha_s^k \ln^{k+m} \frac{\sqrt{s}}{p_\perp}\,, \quad (13)$$

where $\sqrt{s}$ is the total center-of-mass energy and $p_\perp$ is the jet transverse momentum. In inclusive processes, coherence leads to strong cancellations between reals and virtuals so that terms with $m \geq 1$ in Eq. (13) drop out [19, 20]. As a result, for instance, the anomalous dimensions γ^{ij} for the evolution of the space-like jet receive at most single-logarithmic corrections at high energy [20, 21],

$$\gamma^{ij}(\alpha_{\rm s},\omega) = \frac{\alpha_{\rm s}}{\omega^p} c_0^{ij} \left[1 + \sum_{n=1}^{\infty} c_n^{ij} \left(\frac{\alpha_{\rm s}}{\omega}\right)^n + \mathcal{O}\left(\alpha_{\rm s}\left(\frac{\alpha_{\rm s}}{\omega}\right)^{n-1}\right)\right], \qquad (14)$$

where ω is the Mellin moment conjugate to $\ln\sqrt{s}$, p is the leading-order power (dependent on the channel), and c^{ij} are perturbative coefficients. For exclusive jet distributions such cancellations are not present and one may expect stronger enhancements.

The implementation of coherent effects associated with high-energy logarithms is, from the point of view of jet physics, the main motivation for developing the formalism of unintegrated parton distributions and implementing it in shower Monte Carlo. We discuss current work on general aspects of u-pdfs in Sec. 3.

It is worth noting that in the case of small x a gauge-invariant u-pdf definition can be given based on dominance of single gluon polarization at high energy (Fig. 8) [14, 20], because in this case one can relate directly (up to perturbative corrections) the cross-section for a *physical* process (*e.g.*, photoproduction of a heavy-quark pair) to an *unintegrated* gluon distribution, much as one does for deep inelastic scattering in terms of ordinary (integrated) parton distributions[1]. This enables one to treat arbitrarily large transferred momenta (and in particular correctly predict QCD scaling violation at small x [20,26,27])[2]. This ultimately justifies the use of this approach for high-$p_\perp$ processes at the LHC (see *e.g.* Sec. 4 ahead).

A program to perform shower Monte Carlo evolution at unintegrated level has recently been proposed [34], based on two-particle irreducible kernels at the next-to-leading order. The method is based on the generalized ladder expansion [35] first used in [36] for NLO computations of deep inelastic scattering, and then used to treat factorization in the high energy region [20] and in the presence of heavy quark masses [37]. A study of soft-gluon effects in the context of the approach [34] is presented in [38].

[1] On the other hand, it is not obvious how to determine one such relation for general kinematics [22–25]. More discussion of the general case is given in Sec. 3.

[2] Explicit cross-checks *versus* perturbative calculations have been carried out up to next-to-next-to-leading order [28]. This also points to the possible relevance for global analyses of parton evolution [29–31]. See also [32, 33] for recent studies especially in connection with longitudinal structure function measurements.

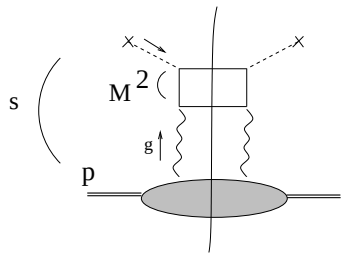

Fig. 8. Unintegrated gluon distribution defined by high energy factorization for $s \gg M^2 \gg \Lambda^2_{\rm QCD}$.

Other existing Monte Carlos based on u-pdfs [39–42] do not attempt to go to NLO accuracy, nevertheless they contain important physics effects at subleading level, see [29,43] for more discussion. Selected applications to jet phenomenology are considered in Sec. 4.

3. Progress in operator approaches to unintegrated pdfs

Fully general factorization formulas for hard-scattering observables in terms of unintegrated parton distributions are yet to be established, and will have a considerably complex structure [24, 44]. A prototypical calculation that illustrates certain main features was carried out in [45] for a specific problem, the electromagnetic form factor of a quark. Although simpler than general hard processes, this case is sufficient to illustrate the role of gauge-invariant operator matrix elements associated with infrared subgraphs in factorization formulas for physical cross-sections.

The technique proposed in [45] to identify these terms is based on gauge-invariant infrared subtractions. Recent analyses of the form factor [46, 47] emphasize the need for subtractions in the context of soft-collinear effective theory [48]. Subtractive techniques [45, 49] serve to treat overlapping momentum regions in studies [50, 51] of transverse momentum dependent factorization[3]. Relations between subtractive techniques in standard perturbative approaches and in soft-collinear effective theory are beginning to be investigated, see for instance [57] and [58][4].

Recent analyses of unintegrated pdf matrix elements along these lines can be found in [63–65] and [66, 67]. Implications for parton-showering methods are considered in [49, 68, 69].

In this section we recall basic aspects of operator matrix elements for unintegrated pdfs and briefly discuss some of the ongoing developments.

[3] Besides collider physics, relevant applications include low-energy cross-sections, *e.g.* semi-inclusive leptoproduction [52–54] and exclusive processes [55, 56].

[4] See also SCET applications to shower algorithms [59], TMD pdfs [60], jet event shapes [61], jets in a dense medium [62] for use of these techniques.

3.1. Gauge invariant matrix elements

The relevance of consistent operator definitions for parton $k_\perp$ distributions was emphasized long ago in the context of Sudakov processes [70], jet physics [71], exclusive production [72], spin physics [73]. The approach commonly used to ensure gauge invariance is to generalize the coordinate-space matrix elements that define ordinary pdf's to the case of field operators at non-lightcone distances. For instance, for the quark distribution one has (Fig. 9)

$$\widetilde{f}(y) = \langle P|\overline{\psi}(y)V_y^\dagger(n)\gamma^+ V_0(n)\psi(0)|P\rangle\,. \tag{15}$$

Here ψ are the quark fields evaluated at distance $y = (0, y^-, y_\perp)$, where $y_\perp$ is in general nonzero, and V are eikonal-line operators in direction n,

$$V_y(n) = \mathcal{P}\exp\left(ig_s\int\limits_0^\infty d\tau n^\mu A_\mu(y+\tau\, n)\right)\,, \tag{16}$$

which we require to make the matrix element gauge-invariant. The unintegrated quark distribution is obtained from the double Fourier transform in y^- and $y_\perp$ of $\widetilde{f}$. An extra gauge link at infinity [74] is to be taken into account in the case of physical gauge.

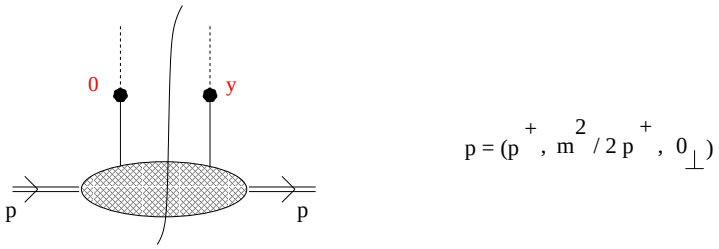

Fig. 9. Correlator of two quark fields at distance y.

There are subtleties, however, to using Eq. (15) beyond tree level. Parton distributions at fixed $k_\perp$ are not protected by KLN cancellation [75] against lightcone divergences near the $x = 1$ endpoint [70,76]. The singularity structure at $x \to 1$ is different than for ordinary (integrated) distributions, giving divergences even in dimensional regularization with an infrared cut-off [63]. The singularities can be understood in terms of gauge-invariant eikonal-line matrix elements [63] and related to cusp anomalous dimensions [66, 77, 78].

This can be analyzed explicitly at one loop. Expansion in powers of y^2 of the coordinate-space matrix element (15) at this order yields a result of the form [63, 79]

$$\widetilde{f}_1(y) \;=\; \frac{\alpha_{\rm s} C_{\rm F}}{\pi}\, p^+ \int\limits_0^1 dv\, \frac{v}{1-v} \left\{ \left[e^{ip\cdot yv} - e^{ip\cdot y} \right] \, \Gamma\left(2-\frac{d}{2}\right) \left(\frac{4\pi\mu^2}{\rho^2}\right)^{2-d/2} \right.$$
$$\left. +\; e^{ip\cdot yv}\; \pi^{2-d/2}\, \Gamma\left(\frac{d}{2}-2\right) (-y^2\mu^2)^{2-d/2} + \cdots \right\}, \qquad (17)$$

where μ is the dimensional-regularization scale and ρ is an infrared mass regulator. The lightcone singularity $v \to 1$, corresponding to the exclusive boundary $x = 1$, cancels for ordinary pdf's (first term in the right hand side of Eq. (17)) but it is present, even at $d \neq 4$ and finite ρ, in subsequent terms. This implies that, using the matrix element (15), the $1/(1-x)$ factors from real emission probabilities do not in general combine with virtual corrections to give $1/(1-x)_+$ distributions, but leave uncancelled divergences at fixed $k_\perp$. It is only after supplying the above matrix element with a regularization prescription that the distribution is well-defined.

Similarly to what observed in [45] for the case of the Sudakov form factor, the choice of a particular regularization method for the lightcone divergences also affects the distributions integrated over $k_\perp$ and the ultraviolet subtractions. The analyses in [63, 68, 80–82] address issues that are concerned precisely with the coefficient functions governing the expansion of unintegrated distributions in terms of ordinary ones. Evolution equations both in mass [6, 53] and in rapidity [51, 71] are implied by (17).

A possible regularization method for the endpoint is by cut-off, implemented by taking the eikonal line n in equation (16) to be non-light-like [51, 64, 70, 71, 83, 84], combined with evolution equations in the cut-off parameter $\eta = (p\cdot n)^2/n^2$ [71, 77]. Then the cut-off in x at fixed $k_\perp$ is of order $1 - x \gtrsim k_\perp/\sqrt{4\eta}$. Monte Carlo generators that make use of unintegrated pdfs can also be regarded as implementing a cut-off. We consider such applications in Sec. 4.

There also exists a more systematic method than the cut-off, based on the subtractive technique of [45, 49]. Although phenomenological studies in this framework are not available yet, this method is potentially relevant both for investigations of parton branching approaches beyond leading logarithms [49, 59, 69] and for addressing issues of factorization [85] and its possible breaking [86–89]. We briefly comment on these potential directions of development in the next two subsections.

3.2. Subtractive method

The cut-off regularization is widely used to treat the endpoint region [51, 64]. It is however not particularly well-suited for applications beyond

leading order. Having introduced $n^2 \neq 0$ as in the previous subsection, the two lightcone limits $y^2 \to 0$ and $n^2 \to 0$ do not necessarily commute. The integral over $k_\perp$ of the distribution has a finite dependence on the regularization parameter η, which makes the relation with the standard operator product expansion not so transparent.

An alternative route is based on the subtractive method [45, 49]. This is reviewed in [44]. The direction n in Eq. (16) in this case is kept to be light-like but the divergences are canceled by multiplicative, gauge-invariant counterterms given by vacuum expectation values of eikonal operators. The counterterms contain in general both light-like and non-light-like eikonals. The matrix element with subtraction factors is pictured schematically in Fig. 10. The graph in the numerator stands for the same matrix element as in Eq. (15), or Fig. 9. The graphs in the denominator represent the counterterms. Here $y = (0, y^-, y_\perp)$, $\bar{y} = (0, y^-, 0_\perp)$, and the eikonal line in direction u is the auxiliary eikonal that provides a gauge-invariant regulator near $x = 1$ and cancels in the matrix element at $y_\perp = 0$ [63].

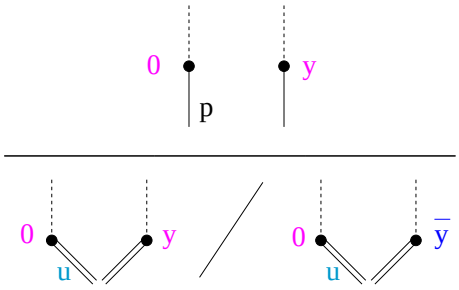

Fig. 10. Matrix element with subtractive regularization.

The form of the counterterms in Fig. 10 is simple in coordinate space, where it can be given in terms of compact all-order expressions. Corresponding expressions are obtained in momentum space by expanding order by order. In particular, it is noted in [63] that at one loop the two counterterms in Fig. 10 give contributions to the unintegrated density $f(x, k_\perp)$ respectively, of the form

$$-W_{\rm R}(x, k_\perp, \zeta) + \delta(1-x)\,\delta(k_\perp) \int dx' dk'_\perp W_{\rm R} \tag{18}$$

and

$$+\delta(k_\perp) \int dk'_\perp W_{\rm R}(x, k'_\perp, \zeta) - \delta(1-x)\,\delta(k_\perp) \int dx' dk'_\perp W_{\rm R}\,, \tag{19}$$

where ζ measures the angle for the eikonal u, and $W_{\rm R}$ is computed to order $\alpha_{\rm s}$. The structure in Eqs. (18), (19) results in a well-prescribed extension for $k_\perp \neq 0$ of the plus-distribution regularization.

For theoretical applications, the subtractive method provides the technique to handle overlapping divergences in infrared regions in factorization studies, see *e.g.* [50, 51]. It has been used to relate the endpoint behavior at fixed $k_\perp$ with the cusp anomalous dimension [66] and investigate the role of the Mandelstam–Leibbrandt prescription in lightcone gauges [67]. For phenomenological applications, the subtractive method is likely more suitable than the cut-off method for using transverse-momentum dependent parton distributions at subleading-log level. It may be helpful for programs of global NLO analyses incorporating Sudakov resummation [90, 91], and in attempts to construct parton-shower algorithms beyond leading order [59, 68].

3.3. Coulomb-phase effects

The treatment of soft gluons exchanged between subgraphs in different collinear directions is crucial in establishing factorization for general cases. The underlying dynamics is that of non-abelian Coulomb phase [85], involving interactions with spectator partons [92]. The issue was studied long ago for fully inclusive Drell–Yan [93]. For more complex observables, including color in both initial and final states, a systematic treatment is still missing. Potential non-universality effects of $k_\perp$-dependent parton distributions [89] are discussed in [86–88] by model calculations for di-hadron and di-jet hadroproduction near the back-to-back region. A typical graph is shown in Fig. 11. Universality-breaking terms potentially appear at high orders of perturbation theory, involving soft gluons coupling initial and final states.

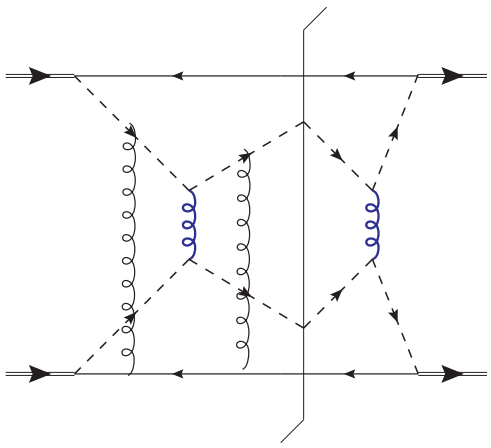

Fig. 11. Soft gluon exchange with spectator partons [87].

Although the role of these corrections is yet to be fully established, it is interesting that Coulomb/radiative mixing terms are also found [94] to be responsible for the breaking of angular ordering in the initial-state cascade and the appearance of superleading logarithms in di-jet cross-sections with a gap in rapidity. A full understanding of these issues will be relevant to clarify the range of validity of the arguments based on the calculations of [86, 87].

4. Applications to jets

This section discusses applications of the unintegrated pdf parton branching to jet physics.

We start by considering a new area of measurements that will open up at the LHC, involving events that are both high-p_{T} and forward. Using the forward calorimeters, experiments will be able to measure azimuthal plane correlations between jets across intervals of five units or more in rapidity.

Then we turn to results for angular and momentum correlations in multi-jet final states observed, at central rapidities, in $p\bar{p}$ and ep collisions. Finally we comment on possible applications to recent measurements of azimuthal distributions in bottom quark jet production at the Tevatron.

4.1. Forward jets in hadronic collisions

Experiments at the LHC will explore the forward region in pp collisions with the main general-purpose detectors and with dedicated experiments, including both proton taggers and forward calorimeters [29, 95–97]. The forward-physics program involves a wide range of topics, from QCD to discovery processes. In particular, owing to the large center-of-mass energy of the collision and the unprecedented experimental coverage, it becomes possible to carry out a program of high-p_{T} physics at very large rapidities.

An example process, forward jet production, is pictured in Fig. 12 [98]. The kinematics of the process is characterized by the large ratio of subenergies $s_2/s_1 \gg 1$, giving rise to potentially large perturbative corrections.

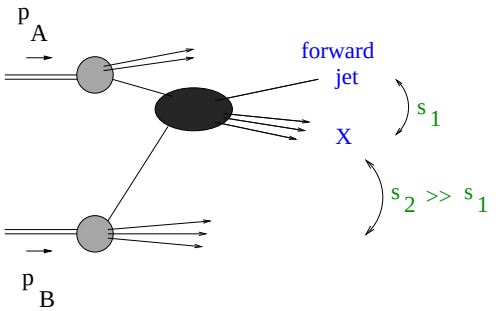

Fig. 12. Production of forward jet in hadron–hadron collisions.

The initial-state parton configurations contributing to forward production are asymmetric, with the parton in the top subgraph being probed near the mass shell and large x, while the parton in the bottom subgraph is off-shell and small-x.

At the LHC it will be possible to observe events where sizeable p_{T}'s are produced several units of rapidity apart, and measure azimuthal plane correlations between jets across rapidity intervals $\Delta\eta \gtrsim 4 \div 6$ [29,95,97]. The jet cross-section differential in transverse energy Q_{t} and azimuthal angle φ can be computed by high-energy factorization [14, 18, 98] as

$$\frac{d\sigma}{dQ_{\mathrm{t}}^2 d\varphi} = \sum_a \int \phi_{a/A} \otimes \frac{d\widehat{\sigma}}{dQ_{\mathrm{t}}^2 d\varphi} \otimes \phi_{g^*/B}\,, \tag{20}$$

where $\widehat{\sigma}$ is the hard scattering cross-section, calculable from a suitable off-shell continuation of perturbative matrix elements, $\phi_{a/A}$ is the distribution of parton a obtained by near-collinear shower evolution, and $\phi_{g^*/B}$ is the gluon unintegrated distribution obtained from $k_\perp$-dependent parton branching.

Potentially significant coherence effects involve both the short-distance factor $\widehat{\sigma}$ and the long-distance factor ϕ. Fig. 13 [98] illustrates the effect in the short distance part. Here we consider the hard scattering function for the term $a = q$ in Eq. (20), and separate the contributions proportional to the color factors C_{F}^2 and $C_{\mathrm{F}}C_{\mathrm{A}}$. The final state transverse energy Q_{t} is defined in terms of the momenta of the two hardest jets, working in the laboratory frame. We plot the cross-section *versus* the ratio between k_{t}, measuring the transverse momentum carried away by additional jets accompanying the two leading jets, and Q_{t}. The leading-order process with two back-to-back jets corresponds to the region $k_{\mathrm{t}}/Q_{\mathrm{t}} \to 0$.

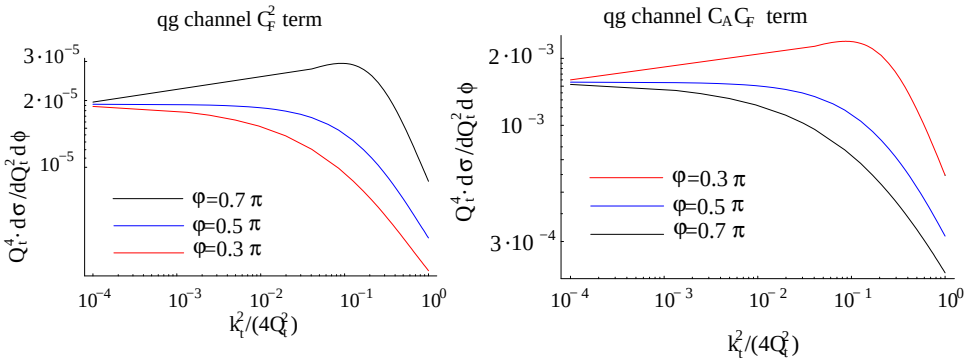

Fig. 13. Off-shell continuation of the qg hard cross-section for forward jet production at high energies [98]: (left) C_{F}^2 term; (right) $C_{\mathrm{F}}C_{\mathrm{A}}$ term.

We observe in Fig. 13 that the role of coherence from multi- gluon emission is to set the dynamical cut-off at values of k_t of order Q_t. Non-negligible effects arise at high energy from the finite-k_t tail. These effects are not included in collinear-branching generators, and become more and more important as the jets are observed at large rapidity separations. Monte Carlo implementations of Eq. (20) and the coherent matrix elements will be relevant for phenomenological studies of the forward region.

To get a handle on what size effects one may expect, it is interesting to ask what one can learn from $p\bar{p}$ and ep data. Most of this data is at central rapidities. Nevertheless, certain correlations among jets in angle and momentum, even in the central region, turn out to give useful information. We turn to this in the next subsection.

4.2. Jet correlations in $p\bar{p}$ and ep final states

In a multi-jet event the correlation in the azimuthal angle $\Delta\phi$ between the two hardest jets provides a useful measurement of how well multiple-radiation effects are described. At the LHC such measurements may become accessible relatively early and be used to test the description of complex hadronic final states by Monte Carlo generators [99].

Data on $\Delta\phi$ correlations are available from the Tevatron [100] and from Hera [101–103]. The comparison with Monte Carlos and perturbative results are very different in the two cases. The Tevatron $\Delta\phi$ distribution (Fig. 14)

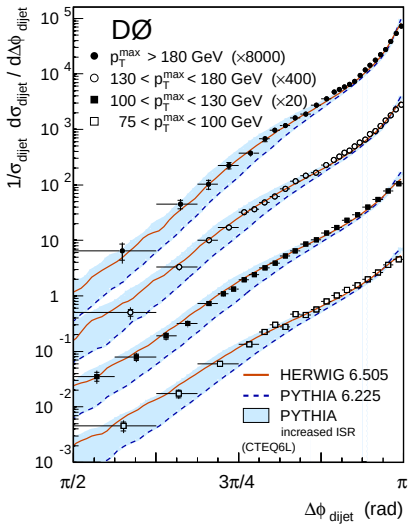

Fig. 14. Dijet azimuthal correlations measured by DØ along with the HERWIG and PYTHIA results [100].

drops by about two orders of magnitude over a fairly narrow range, essentially still close to the two-jet region. The measurement is dominated by leading-order processes, with small sub-leading corrections. Data are reasonably well described both by collinear showers (HERWIG and the new tuning of PYTHIA) and by fixed-order NLO calculations [99, 100].

The Hera $\Delta\phi$ measurements, on the other hand, are much more sensitive to higher orders, Fig. 15 [101]. NLO results for di-jet azimuthal distributions are affected by large corrections [104]) in the small-$\Delta\phi$ and small-x region, and begin to fall below the data for three-jet distributions in the smallest $\Delta\phi$ bins [101]. These measurements are characterized by large phase-space available for jet production and are relevant for extrapolation of initial-state showering effects to the LHC.

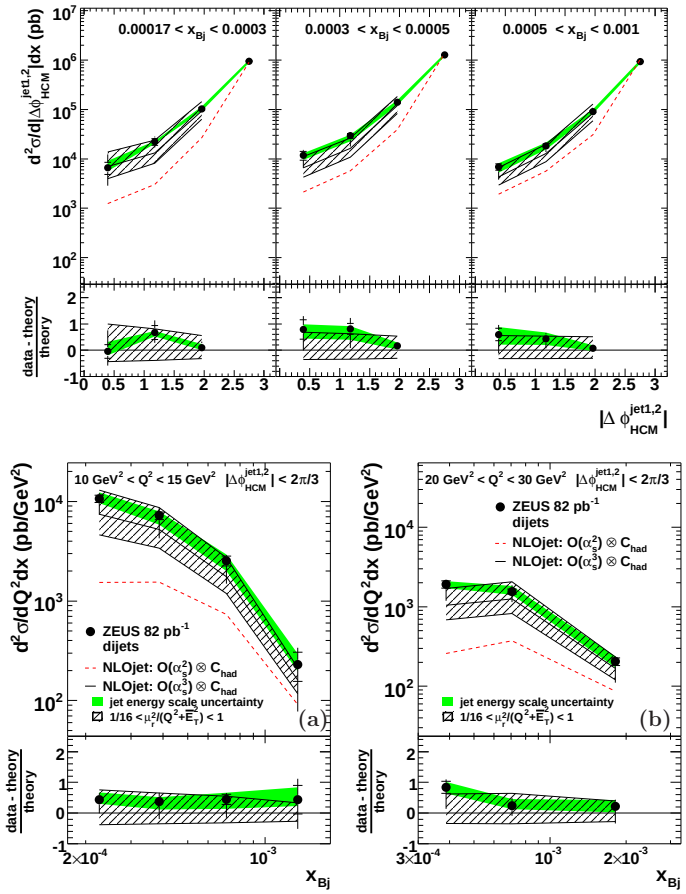

Fig. 15. (Up) Azimuth dependence and (bottom) Bjorken-x dependence of ep di-jet distributions [101], compared with NLO results.

Refs. [43, 105] investigate the effects of corrections to collinear-ordered showers on angular and momentum correlations, Fig. 16. The shape of the distributions is different for HERWIG and for the $k_\perp$-shower Monte Carlo CASCADE, with the largest differences occurring at small $\Delta\phi$ and small $\Delta p_{\rm t}$, where the two highest $E_{\rm T}$ jets are not close to back to back [106] and one has effectively three hard, well-separated jets. Ref. [43] also analyzes the angular distribution of the third jet and finds significant contributions from regions where the transverse momenta in the initial state shower are not ordered. The description of the measurement by the $k_\perp$-shower is good, whereas the collinear-based shower is not sufficient to describe it.

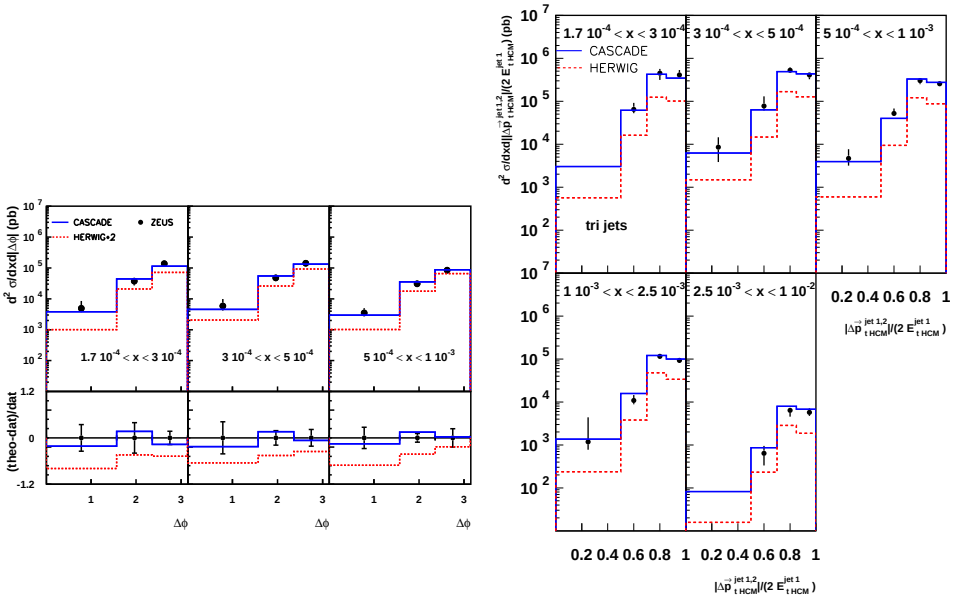

Fig. 16. (Left) angular correlations and (right) momentum correlations [43] in three-jet final states measured by [101], compared with $k_\perp$-shower (CASCADE) and collinear-shower (HERWIG) Monte Carlo results.

Fig. 17 illustrates the relative contribution of matrix element corrections and shower evolution to the result [43]. The solid red curve is the full result, normalized to the back-to-back cross-section. The dashed blue curve is obtained from the same unintegrated pdf's but by taking the collinear approximation in the hard matrix element. The dashed curve drops much faster than the full result as $\Delta\phi$ decreases, indicating that the high-$k_\perp$ component in the hard ME is necessary to describe jet correlations for small $\Delta\phi$. The dotted (violet) curve is the result obtained from the unintegrated pdf without any resolved branching. This represents the contribution of the intrinsic

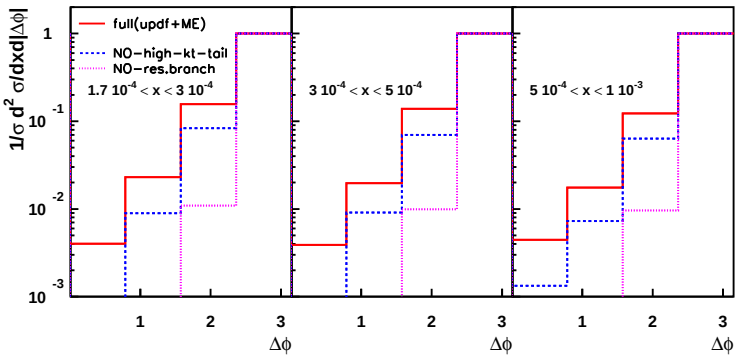

Fig. 17. The dijet azimuthal distribution [43] normalized to the back-to-back cross-section: (solid red) full result (u-pdf $\oplus$ ME); (dashed blue) no finite-$k_\perp$ correction in ME (u-pdf $\oplus$ ME$_{\text{collin.}}$); (dotted violet) u-pdf with no resolved branching.

$k_\perp$ distribution only, corresponding to nonperturbative, predominantly low-$k_\perp$ modes. That is, in the dotted (violet) curve one retains an intrinsic $k_\perp \neq 0$ but no effects of coherence. We see that the resulting jet correlations in this case are down by an order of magnitude. The inclusion of the perturbatively computed high-$k_\perp$ correction distinguishes the calculation [43] of multi-jet cross-sections from other shower approaches (see *e.g.* [42]) that include transverse momentum dependence in the pdfs but not in the matrix elements.

4.3. b-jets correlations

Measurements of angular correlations have recently been performed for bottom quark jet production at the Tevatron [107–109]. See [29, 110, 111] for reviews of related phenomenology.

Results for b-jet distributions in invariant mass and azimuthal angle are shown in Fig. 18 [108] and Fig. 19 [109]. Collinear-shower descriptions of the data do not appear to be satisfactory especially at small $\Delta\phi$ [1]. The measurements are sensitive to soft underlying events [108] and in this respect parton showers using unintegrated densities are likely to provide a more natural framework [113] to describe the $k_\perp$ distribution of the underlying event. Phenomenological studies of b-jet correlations based on $k_\perp$-dependent parton branching are warranted.

As regards small $\Delta\phi$, it is worth recalling that heavy flavor hadroproduction is dominated for sufficiently high energies by gluon splitting into heavy-quark pairs [14], $g \to Q\overline{Q}$ where g is produced from the spacelike jet. The coefficient functions associated to the leading high-energy singularity [14] enhance regions that are not ordered in transverse momentum in the

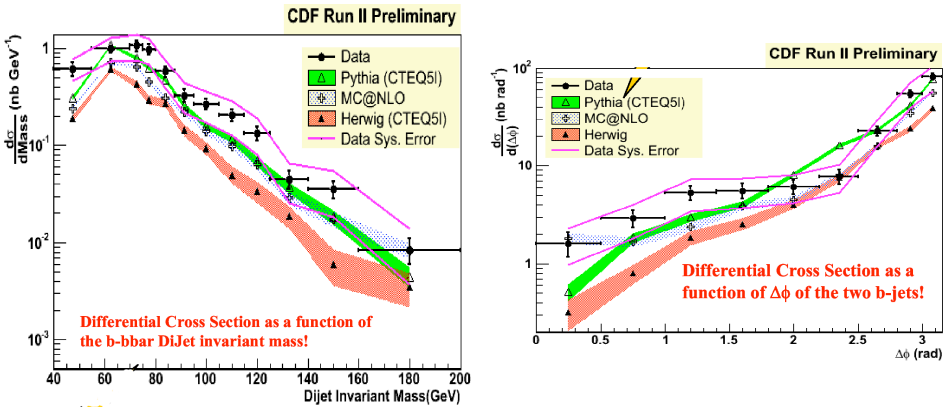

Fig. 18. Invariant-mass distribution and azimuthal-angle distribution for production of b-jets at the Tevatron [108].

initial state jet. In fact, such contributions are already found to be significant at the level of the NLO correction [111, 112]. They may be related to the rather large theoretical uncertainties, due to uncalculated higher orders, found [111, 112] in the NLO predictions when going from the Tevatron to the LHC. It will be of interest to investigate their role for the shape of the $\Delta\phi$ distribution.

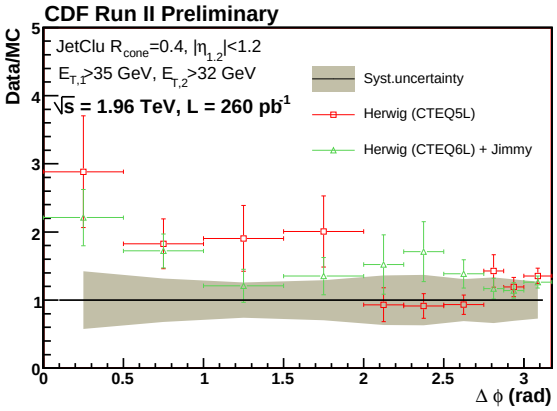

Fig. 19. Comparison of data and Monte Carlos for b-jet azimuthal correlations at the Tevatron [109].

Note that even more complex multi-scale effects are expected [29] at the LHC in the associated production of bottom quark pairs and W/Z bosons [114], and possibly in final states with Higgs bosons [115–117] especially for measurements of the less inclusive distributions and correlations.

Similar studies are to be carried out in vector boson production, probing sea-quark channels [20, 118, 119] at high energy. This is relevant for early phenomenology at the LHC, as the possible broadening of W and Z p_{T} distributions [120] affects the use of these processes as luminosity monitor [121].

I thank the organizers for inviting me to participate in this conference commemorating Jan Kwieciński.

REFERENCES

[1] B.R. Webber, CERN Academic Training Lectures (2008).

[2] R.K. Ellis, W.J. Stirling, B.R. Webber, *QCD and Collider Physics*, CUP, 1996.

[3] J.C. Collins, D.E. Soper, G. Sterman, *Adv. Ser. Direct. High Energy Phys.* **5**, 1 (1988).

[4] M.H. Seymour, Lectures at CTEQ School (2006).

[5] S. Frixione, CERN Academic Training Lectures (2006).

[6] A. Bassetto, M. Ciafaloni, G. Marchesini, *Phys. Rep.* **100**, 201 (1983).

[7] Yu.L. Dokshitzer, V.A. Khoze, A.H. Mueller, S.I. Troian, *Perturbative QCD*, Ed. Frontieres, Gif-sur-Yvette (1991).

[8] V.N Gribov, *Sov. J. Nucl. Phys.* **5**, 399 (1967); F.E. Low, *Phys. Rev.* **110**, 974 (1958).

[9] J. Frenkel, J.C. Taylor, *Nucl. Phys.* **B246**, 231 (1984); R. Doria, J. Frenkel, J.C. Taylor, *Nucl. Phys.* **B168**, 93 (1980).

[10] B.R. Webber, *Annu. Rev. Nucl. Part. Sci.* **36**, 253 (1986).

[11] Yu.L. Dokshitzer, V.A. Khoze, A.H. Mueller, S.I. Troian, *Rev. Mod. Phys.* **60**, 373 (1988).

[12] M. Ciafaloni, in *Perturbative Quantum Chromodynamics*, Ed. A.H. Mueller, World Scientific, Singapore 1989.

[13] M. Ciafaloni, *Nucl. Phys.* **B296**, 49 (1988).

[14] S. Catani, M. Ciafaloni, F. Hautmann, *Phys. Lett.* **B242**, 97 (1990); *Nucl. Phys.* **B366**, 135 (1991).

[15] S. Catani, F. Fiorani, G. Marchesini, *Nucl. Phys.* **B336**, 18 (1990).

[16] G. Marchesini, B.R. Webber, *Nucl. Phys.* **B386**, 215 (1992).

[17] B. Andersson, G. Gustafson, J. Samuelsson, *Nucl. Phys.* **B467**, 443 (1996).

[18] M. Ciafaloni, *Phys. Lett.* **B429**, 363 (1998).

[19] T. Jaroszewicz, *Phys. Lett.* **B116**, 291 (1982).

[20] S. Catani, F. Hautmann, *Nucl. Phys.* **B427**, 475 (1994); *Phys. Lett.* **B315**, 157 (1993).

[21] V.S. Fadin, L.N. Lipatov, *Phys. Lett.* **B429**, 127 (1998); G. Camici, M. Ciafaloni, *Phys. Lett.* **B430**, 349 (1998).

[22] J.R. Andersen *et al., Eur. Phys. J.* **C35**, 67 (2004).

[23] J.C. Collins, hep-ph/0106126.

[24] J.C. Collins, talk at the Light Cone 2008 Workshop, Mulhouse, July 2008; arXiv:0808.2665[hep-ph].

[25] F. Hautmann, H. Jung, *Nucl. Phys. Proc. Suppl.* **184**, 64 (2008) [arXiv:0712.0568[hep-ph]; arXiv:0808.0873[hep-ph].

[26] G. Altarelli, R. Ball, S. Forte, arXiv:0901.1294[hep-ph]; *Nucl. Phys.* **B799**, 199 (2008); M. Ciafaloni, D. Colferai, G.P. Salam, A. Stasto, *J. High Energy Phys.* **0708**, 046 (2007); M. Ciafaloni, D. Colferai, *J. High Energy Phys.* **0509**, 069 (2005).

[27] R.S. Thorne, *Phys. Rev.* **D60**, 054031 (1999); R.K. Ellis, F. Hautmann, B.R. Webber, *Phys. Lett.* **B348**, 582 (1995); J. Kwiecinski, *Z. Phys.* **C29**, 561 (1985).

[28] S. Moch, J.A.M. Vermaseren, A. Vogt, *Phys. Lett.* **B606**, 123 (2005); *Nucl. Phys.* **B691**, 129 (2004).

[29] H. Jung *et al.*, arXiv:0903.3861[hep-ph].

[30] A.D. Martin, W.J. Stirling, R.S. Thorne, G. Watt, 0901.0002[hep-ph].

[31] R.S. Thorne, arXiv:0902.4820[hep-ph].

[32] K. Golec-Biernat, A.M. Stasto, arXiv:0905.1321[hep-ph].

[33] F. Hautmann, arXiv:0812.2873[hep-ph].

[34] S. Jadach, M. Skrzypek, arXiv:0905.1399[hep-ph].

[35] W. Zimmermann, *Ann. Phys.* **77**, 536 (1973).

[36] G. Curci, W. Furmanski, R. Petronzio, *Nucl. Phys.* **B175**, 27 (1980).

[37] J.C. Collins, *Phys. Rev.* **D58**, 094002 (1998).

[38] M. Slawinska, A. Kusina, arXiv:0905.1403[hep-ph].

[39] H. Jung, *Comput. Phys. Commun.* **143**, 100 (2002).

[40] L. Lönnblad, M. Sjödahl, *J. High Energy Phys.* **0402**, 042 (2004).

[41] K. Golec-Biernat, S. Jadach, W. Placzek, P. Stephens, M. Skrzypek, *Acta Phys. Pol. B* **38**, 3149 (2007).

[42] S. Höche, F. Krauss, T. Teubner, *Eur. Phys. J.* **C58**, 17 (2008).

[43] F. Hautmann, H. Jung, *J. High Energy Phys.* **0810**, 113 (2008).

[44] J.C. Collins, *Acta Phys. Pol. B* **34**, 3103 (2003).

[45] J.C. Collins, F. Hautmann, *Phys. Lett.* **B472**, 129 (2000).

[46] J. Chiu, A. Fuhrer, A.H. Hoang, R. Kelley, A.V. Manohar, [arXiv:0901.1332[hep-ph]].

[47] J. Chiu, A. Fuhrer, A.H. Hoang, R. Kelley, A.V. Manohar, [arXiv:0905.1141[hep-ph]].

[48] A.V. Manohar, I.W. Stewart, *Phys. Rev.* **D76**, 074002 (2007).

[49] J.C. Collins, F. Hautmann, *J. High Energy Phys.* **0103**, 016 (2001); F. Hautmann, *Nucl. Phys.* **B604**, 391 (2001); hep-ph/9708496.

[50] J.C. Collins, A. Metz, *Phys. Rev. Lett.* **93**, 252001 (2004).

[51] X. Ji, J. Ma, F. Yuan, *Phys. Rev.* **D71**, 034005 (2005); *J. High Energy Phys.* **0507**, 020 (2005).

[52] M. Anselmino *et al.*, `arXiv:0807.0173[hep-ph]`; M. Anselmino *et al., Phys. Rev.* **D71**, 074006 (2005).

[53] F. Ceccopieri, L. Trentadue, *Phys. Lett.* **B660**, 43 (2008).

[54] A. Bacchetta, D. Boer, M. Diehl, P.J. Mulders, *J. High Energy Phys.* **0808**, 023 (2008).

[55] K. Goeke, S. Meissner, A. Metz, M. Schlegel, *J. High Energy Phys.* **0808**, 038 (2008).

[56] A.V. Efremov, P. Schweitzer, O.V. Teryaev, P. Zavada, `[arXiv:0903.3490[hep-ph]]`.

[57] C. Lee, G. Sterman, *Phys. Rev.* **D75**, 014022 (2007).

[58] A. Idilbi, T. Mehen, *Phys. Rev.* **D76**, 094015 (2007); *Phys. Rev.* **D75**, 114017 (2007).

[59] C.W. Bauer, F.J. Tackmann, J. Thaler, *J. High Energy Phys.* **0812**, 011 (2008); *J. High Energy Phys.* **0812**, 010 (2008).

[60] J. Chay, `arXiv:0711.4295[hep-ph]`.

[61] M.D. Schwartz, *Phys. Rev.* **D77**, 014026 (2008); M. Trott, *Phys. Rev.* **D75**, 054011 (2007).

[62] A. Idilbi, A. Majumder, `arXiv:0808.1087[hep-ph]`.

[63] F. Hautmann, *Phys. Lett.* **B655**, 26 (2007).

[64] J.C. Collins, T.C. Rogers, A.M. Stasto, *Phys. Rev.* **D77**, 085009 (2008).

[65] T.C. Rogers, *Phys. Rev.* **D78**, 074018 (2008); `arXiv:0712.1195[hep-ph]`, in Proceedings of the RADCOR2007 Symposium.

[66] I.O. Cherednikov, N.G. Stefanis, *Nucl. Phys.* **B802**, 146 (2008); *Phys. Rev.* **D77**, 094001 (2008); `arXiv:0711.1278[hep-ph]`.

[67] I.O. Cherednikov, N.G. Stefanis, `arXiv:0904.2727[hep-ph]`.

[68] J.C. Collins, X. Zu, *J. High Energy Phys.* **0503**, 059 (2005).

[69] J.C. Collins, *Phys. Rev.* **D65**, 094016 (2002).

[70] J.C. Collins, in *Perturbative Quantum Chromodynamics*, Ed. A.H. Mueller, World Scientific, 1989, p. 573.

[71] J.C. Collins, D.E. Soper, *Nucl. Phys.* **B193**, 381 (1981).

[72] S.J. Brodsky, G.P. Lepage, in *Perturbative Quantum Chromodynamics*, Ed. A.H. Mueller, World Scientific, 1989, p. 93.

[73] P. Mulders, R.D. Tangerman, *Nucl. Phys.* **B461**, 197 (1996); D. Boer, P. Mulders, *Phys. Rev.* **D57**, 5780 (1998).

[74] A.V. Belitsky, X. Ji, F. Yuan, *Nucl. Phys.* **B656**, 165 (2003).

[75] T. Kinoshita, *J. Math. Phys.* **3**, 650 (1962); T.D. Lee, M. Nauenberg, *Phys. Rev.* **133**, 1549 (1964).

[76] S.J. Brodsky, D.S. Hwang, B.Q. Ma, I. Schmidt, *Nucl. Phys.* **B593**, 311 (2001).

[77] G.P. Korchemsky, A. Radyushkin, *Phys. Lett.* **B279**, 359 (1992).

[78] G.P. Korchemsky, G. Marchesini, *Phys. Lett.* **B313**, 433 (1993).

[79] F. Hautmann, arXiv:0708.1319[hep-ph].

[80] A.D. Martin, M.G. Ryskin, G. Watt, *Eur. Phys. J.* **C31**, 73 (2003); M.A. Kimber, A.D. Martin, M.G. Ryskin, *Phys. Rev.* **D63**, 114027 (2001).

[81] J. Kwiecinski, A.D. Martin, P.J. Sutton, *Phys. Rev.* **D52**, 1445 (1995).

[82] S. Catani, M. Ciafaloni, F. Hautmann, *Phys. Lett.* **B307**, 147 (1993).

[83] G.P. Korchemsky, *Phys. Lett.* **B220**, 62 (1989).

[84] P. Chen, A. Idilbi, X. Ji, *Nucl. Phys.* **B763**, 183 (2007).

[85] S. Mert Aybat, G. Sterman, *Phys. Lett.* **B671**, 46 (2009).

[86] W. Vogelsang, F. Yuan, *Phys. Rev.* **D76**, 094013 (2007).

[87] J.C. Collins, arXiv:0708.4410[hep-ph].

[88] C.J. Bomhof, P.J. Mulders, *Nucl. Phys.* **B795**, 409 (2008).

[89] C.J. Bomhof, P.J. Mulders, F. Pijlman, *Eur. Phys. J.* **C47**, 147 (2006).

[90] C.P. Yuan, talk at DIS07 Workshop, Munich, April 2007.

[91] P.M. Nadolsky, N. Kidonakis, F.I. Olness, C.P. Yuan, *Phys. Rev.* **D67**, 074015 (2003).

[92] D. Boer, S.J. Brodsky, D.S. Hwang, *Phys. Rev.* **D67**, 054003 (2003).

[93] J.C. Collins, D.E. Soper, G. Sterman, *Nucl. Phys.* **B308**, 833 (1988).

[94] J.R. Forshaw, M.H. Seymour, arXiv:0901.3037[hep-ph]; J.R. Forshaw, A. Kyrieleis, M.H. Seymour, *J. High Energy Phys.* **0608**, 059 (2006).

[95] M. Grothe, arXiv:0901.0998[hep-ex], and references therein.

[96] M.G. Albrow *et al.*, FP420 Coll., arXiv:0806.0302[hep-ex].

[97] CMS Coll., CERN-LHCC-2006-001 (2006); CMS PAS FWD-08-001 (2008).

[98] M. Deak, F. Hautmann, H. Jung, K. Kutak, to appear; F. Hautmann, talk at Rencontres de Moriond, La Thuile (March 2009).

[99] M.G. Albrow *et al.* [TeV4LHC QCD Working Group], hep-ph/0610012.

[100] V.M. Abazov *et al.* [DØ Collaboration], *Phys. Rev. Lett.* **94**, 221801 (2005) [arXiv:hep-ex/0409040].

[101] S. Chekanov *et al.* [ZEUS Collaboration], *Nucl. Phys.* **B786**, 152 (2007) [arXiv:0705.1931[hep-ex]].

[102] M. Hansson, in Proceedings of the 14th International Workshop on Deep Inelastic Scattering DIS2006 Tsukuba, April 2006, p. 539.

[103] A. Aktas *et al.* [H1 Collaboration], *Eur. Phys. J.* **C33**, 477 (2004) [arXiv:hep-ex/0310019].

[104] Z. Nagy, Z. Trocsanyi, *Phys. Rev. Lett.* **87**, 082001 (2001).

[105] F. Hautmann, H. Jung, arXiv:0804.1746[hep-ph], in Proceedings of the 8th International Symposium on Radiative Corrections RADCOR2007.

[106] A. Banfi, M. Dasgupta, Y. Delenda, *Phys. Lett.* **B665**, 86 (2008).

[107] [CDF Collaboration], *Phys. Rev.* **D71**, 092001 (2005); *Phys. Rev.* **D78**, 072005 (2008).

[108] R.D. Field, talk at Monte Carlo Workshop, Hamburg 2007.

[109] [CDF Collaboration], FNAL 8939 (2007).

[110] J. Baines *et al.*, `hep-ph/0601164`.

[111] P. Nason *et al.*, `hep-ph/0003142`.

[112] S. Frixione, P. Nason, B.R. Webber, *J. High Energy Phys.* **0308**, 007 (2003) [`arXiv:hep-ph/0305252`].

[113] G. Gustafson, talk at Desy Workshop, Hamburg, March 2007; G. Gustafson, L. Lönnblad, G. Miu, *J. High Energy Phys.* **0209**, 005 (2002).

[114] M.L. Mangano, *Nucl. Phys.* **B405**, 536 (1993).

[115] F. Hautmann, *Phys. Lett.* **B535**, 159 (2002).

[116] A. Kulesza, G. Sterman, W. Vogelsang, *Phys. Rev.* **D69**, 014012 (2004).

[117] S. Marzani, R.D. Ball, V. Del Duca, S. Forte, A. Vicini, *Nucl. Phys.* **B800**, 127 (2008); A.V. Lipatov, N.P. Zotov, `arXiv:0905.1894[hep-ph]`.

[118] R.D. Ball, S. Marzani, *Nucl. Phys.* **B814**, 246 (2009).

[119] M. Dasgupta, Y. Delenda, *J. High Energy Phys.* **0608**, 080 (2006).

[120] F.I. Olness, talk at HERA-LHC Workshop, CERN, May 2008; S. Berge, P.M. Nadolsky, F.I. Olness, C.P. Yuan, `hep-ph/0508215`.

[121] A.M. Cooper-Sarkar, `arXiv:0707.1593[hep-ph]`.